isvr Institute of Sound and Vibration Research

Sound Power Flux Measurements in Strongly Excited Flow Ducts

K.R. Holland, P.O.A.L. Davies and D.C. van der Walt

ISVR Technical Report No 291

December 2000

University of Southampton

SCIENTIFIC PUBLICATIONS BY THE ISVR

Technical Reports are published to promote timely dissemination of research results by ISVR personnel. This medium permits more detailed presentation than is usually acceptable for scientific journals. Responsibility for both the content and any opinions expressed rests entirely with the author(s).

Technical Memoranda are produced to enable the early or preliminary release of information by ISVR personnel where such release is deemed to the appropriate. Information contained in these memoranda may be incomplete, or form part of a continuing programme; this should be borne in mind when using or quoting from these documents.

Contract Reports are produced to record the results of scientific work carried out for sponsors, under contract. The ISVR treats these reports as confidential to sponsors and does not make them available for general circulation. Individual sponsors may, however, authorize subsequent release of the material.

Sound Power Flux Measurements in Strongly Excited Flow Ducts

K R Holland, P O A L Davies and D C van der Walt

ISVR Technical Report No. 291

December 2000

UNIVERSITY OF SOUTHAMPTON

INSTITUTE OF SOUND AND VIBRATION RESEARCH

FLUID DYNAMICS AND ACOUSTICS GROUP

Sound Power Flux Measurements in Strongly Excited Flow Ducts

by

K R Holland, P O A L Davies and D C van der Walt

ISVR Technical Report No. 291

December 2000

Authorized for issue by
Professor P A Nelson
Group Chairman

ACKNOWLEDGEMENTS

The laboratory experiments form part of the studies of flow-induced pressure pulsations in pipe systems transporting compressible fluids supported by the Engineering and Physical Sciences Research Council grant K79994. Thanks are due to Bosal Afrika for their financial support of the investigations by the third author.

CONTENTS

FIGURES

Figure 1 Phase of cross spectrum in exhaust tailpipe.

Figure 2 Single shot sample spectrum - only highlighted lines contribute to averaging - signal-to-noise ratio 0 dB.

Figure 3 Comparison of measurements with flow Mach number 0.1. (a) With swept sine excitation and selective averaging; (b) with White noise excitation. (1) Transfer function $\hat{H}_{12}$, — Mod - - Phase; (2) coherence; (3) autospectrum at microphone #1, — with acoustic excitation - - flow only.

Figure 4(a) Experimental set up used for the measurements on the vehicle.

Figure 4(b) Mass flow (circles), inlet temperature (thick solid), outlet temperature (thick dash), inlet Mach number (thin dash) and outlet Mach number (thin solid) recorded for the Honda 1.5 litre during a full throttle run up on the chassis dynamometer.

Figure 5 Normalised acoustic power flux in the tailpipe at Mach number M = 0.2, (a) low flow noise system, (b) high flow noise system; ——, measured; ----, predicted.

Figure 6 Radiated acoustic power at Mach number M = 0.2, (a) low flow noise system, (b) high flow noise system; ——, measured; ----, predicted from tailpipe power flux.

Figure 7 Measured power flux in tailpipe at M = 0.1, sound sources switched off; ——, coherent; ----, total.

Figure 8 Radiated coherent power; with "noisy" chamber at M = 0.2; ——, measured in free field; ----, predicted from tailpipe power flux.

Figure 9 Measured (thin dash) and predicted (solid) normalised acoustic power flux in the outlet pipe for a full throttle run up of the Honda 1.5 litre.

Figure 10 Sound pressure orders measured at station #1 for the Honda 1.5 litre during a full throttle run up on the chassis dynamometer, 2E (thick solid), 4E (thin solid), 6E (thin dash), 8E (thick dash).

ABSTRACT

This contribution describes new robust procedures for the measurement of sound power flux at appropriate axial positions along a flow duct, using pairs of flush wall mounted microphones, or pressure transducers. The technology includes the application of selective averaging [1], order tracking and optimised sampling rate methods to identify the small fraction of the total fluctuating wave energy that is being propagated along the flow path in a reverberent, or highly reactive duct system. Such measurements can also be used to quantify the local acoustic characteristics that govern the generation, transfer and propagation of wave energy in the system. Illustrative examples include the determination of the acoustic characteristics of individual silencing elements installed in IC engine intakes and exhausts both on the flow bench and during controlled acceleration or run down on a test bed, where the wave component spectral levels approached 170 dB.

SYMBOLS AND ABBREVIATIONS

a	duct radius
c	speed of sound
d	pipe internal diameter
f	cyclic frequency
$\hat{G}_{12}$	cross-power spectrum $\hat{p}_1^* . \hat{p}_2$
G_{11}	autospectrum $\hat{p}_1^* . \hat{p}_1$
$\hat{H}_{12}$	transfer function $\hat{p}_2 / \hat{p}_1$
I	acoustic intensity
k	wavenumber ω_0 / c
l	transducer spacing
M	Mach number u_0 / c_0
p	pressure
$\hat{p}$	spectral pressure component, complex amplitude
$\hat{p}^+, \hat{p}^-$	positively and negatively travelling acoustic component wave amplitudes
R	pressure reflection coefficient $\hat{p}^- / \hat{p}^+$
t	time
S	surface, cross-section area
s	fluctuating entropy
u	velocity
u_i	acoustic velocity component
U_i	time averaged flow velocity component
v_i	fluctuating solenoidal velocity component
W	acoustic power flux
α	viscothermal attenuation coefficient
ρ	fluid density
ω	radian frequency $2\pi f$

Subscripts

a	acoustic, isentropic
0	ambient value
s	solenoidal

1. INTRODUCTION

Compliance with legislation and other directives restricting the permissible levels of sound emission is normally demonstrated by performing appropriate sound power measurements [1]. The major contribution to traffic noise by both engine intake and exhaust is widely recognised, while similar flow generated noise often contributes significantly to emissions from industrial plant, domestic equipment or other activities. The development and validation of appropriate noise control strategies also requires appropriate sound power measurements, while these also feature widely in methodologies [2] for the acoustic design and refinement of quality products. This includes the assessment of the acoustic properties of the individual components with their contribution to the overall performance of the system under operational conditions. The techniques described here assume one dimensional acoustic wave propagation and have already been experimentally validated [1] with periodic excitation up to a sound pressure level (SPL) of around 130 dB. The measurements described here concern fluctuating pressure levels from one to two orders of magnitude in excess of this value, thus extending their successful application to conditions commonly experienced in practice.

In an ideal acoustic medium at rest, the sound power crossing any closed surface S is defined [3] as

$$W = \int_S I_i dS_i \,, \tag{1}$$

where $I_i =< p_a u_i >, i = 1,2,3,$ are the components of the time averaged acoustic intensity vector, p_a is the fluctuating acoustic pressure and u_i the corresponding acoustic velocity components in the isentropic irrotational fluid motion associated with the acoustic wave. In a moving acoustic medium, Morfey [3] showed that the corresponding components of the acoustic energy flux per unit area are expressed by

$$I_i =< p_a u_i > + \frac{U_i}{\rho_0 c_0^2} < p_a^2 > + \frac{U_i U_j}{c_0^2} < p_a u_j > + \rho_0 U_j < u_i u_j >, \tag{2}$$

where U_i, U_j are the time averaged components of the flow velocity and ρ_0, c_0 are respectively the ambient density and sound speed.

1.1 Sound power flux in flow ducts

Flow duct geometry is normally complex and consists of lengths of uniform pipe connecting other system components such as expansions, contractions, resonators, branches and so on. Flow duct acoustic behaviour is usually highly reactive, while wave reflection at the junctions between elements [4-6], with interference between the resulting incident and reflected waves results in an acoustic field consisting of both standing and progressive waves. As well as acoustic disturbances propagating at the speed of sound, the fluid motion generally includes other disturbances convecting with the flow. These represent turbulent and vortical motion generated at the duct boundaries or cast off [4, 6] with separating flow, and include fluctuating velocity components v_i and entropy s with their associated pressure and density fluctuations p_s and ρ_s. Thus, for example, sound power measurements require appropriate experimental procedures [4-6] that isolate or identify the acoustic contribution $p_a(t)$ in the observed pressure time history $p'(t) = p_a(t) + p_s(t)$. Furthermore, as well as such contamination, the systematic axial distribution of acoustic pressure and velocity amplitude associated

with the standing waves may result in adverse signal to noise ratios for sequences of specific frequencies, at one or more axial positions along each pipe.

Sets of examples are presented here describing the application of robust procedures yielding reliable estimates of the net sound power flux associated with one dimensional wave motion under strongly reactive conditions in flow ducts. These show that appropriate cross-power spectral analysis of the signals acquired simultaneously from a sequence of pairs of flush wall mounted pressure transducers can be processed [1, 4-7] to establish the acoustic characteristics of each system element of interest. From these one can calculate the small proportion of the total fluctuating wave energy that is being propagated through it. The appropriate procedures differed somewhat with each application, which included strong acoustic excitation by an acoustic driver [1], aeroacoustic excitation produced by the flow alone [8] and finally by the exhaust process of a petrol engine [9] accelerating on a test bed. A common representative geometry, consisting of an expansion chamber with its inlet and outlet pipes was chosen for each case.

Acoustic energy propagation is restricted to one dimensional wave motion below the cut off frequency at which higher order modes decay exponentially. In a pipe with radius a this corresponds to a Helmholtz number $ka = 1.84(1-M^2)^{0.5}$ where M is the mean flow Mach number u_0 / c_0. This limit corresponds to 2000 Hz in a 100 mm diameter pipe. Provided the frequency range of interest lies below such limits, this restriction to plane wave motion offers a considerable simplification to both measurement procedures and to their subsequent analysis. For example, the measurement [10] of the acoustic characteristics of the first two propagating circumferential modes in a 300 mm diameter duct just above "cut on" at frequencies of 646 and 1072 Hz respectively, required an array of eight pairs of flush wall mounted microphones.

2. SOUND POWER FLUX MEASUREMENTS IN FLOW DUCTS

With one dimensional acoustic wave motion (plane waves) travelling along a uniform pipe the amplitude of each spectral component of the acoustic pressure p_a and velocity u_a is related to the corresponding amplitude of the incident $\hat{p}^+$ and reflected $\hat{p}^-$ component waves [5], at a mean flow Mach number M by

$$\hat{p}_a = \hat{p}^+ + \hat{p}^- \quad , \quad \rho_0 c_0 \, \hat{u}_a = \hat{p}^+ - \hat{p}^- \qquad \text{(3a, b)}$$

where equation (3a) is always true and (3b) remains a close approximation for $M > 0$ [5], so long as the influence of viscothermal attenuation remains sufficiently small. After substitution from equations (3), equation (2) describing the acoustic intensity simplifies [4, 5] to

$$I = I^+ - I^- = [\,|\,\hat{p}^+\,|^2\,(1+M)^2 - |\,\hat{p}^-\,|^2\,(1-M)^2\,] / \rho_0 c_0 , \qquad (4)$$

where I^+ and I^- are respectively the incident and reflected components of the spectral acoustic intensity I.

2.1 Extraction of the $\hat{p}^+, \hat{p}^-$ spectra from the transducer signals

Consider the two pressure time histories measured by transducers at positions 1 and 2 an axial distance l apart. The corresponding acoustic contributions to the pressure spectra derived from the signals recorded at the two positions are related by [1, 4-7]

$$\hat{p}_1(\omega) = \hat{p}_1^+(\omega) + \hat{p}_1^-(\omega)\,, \quad \hat{p}_2(\omega) = \hat{p}_1^+ \exp(-jk^+l) + \hat{p}_1^- \exp(jk^-l)\,, \qquad \text{(5a, b)}$$

where $k^{\pm}$ are the corresponding wavenumbers given by $(\omega/c + \alpha(1-j)/(1 \pm M)$ respectively and α is the viscothermal attenuation coefficient [1,5]. If the cross-spectrum estimated from the pressure-time histories at positions 1 and 2 is $\hat{G}_{12}$, while G_{11} and G_{22} are the corresponding autospectra, one can show that the acoustic pressure reflection coefficient spectrum $\hat{R}_1$ defined as the ratio $\hat{p}_1^- / \hat{p}_1^+$ is also [1] expressed by

$$\hat{R}_1 = -[\hat{G}_{12} - G_{11}\exp(-jk^+l)]/[\hat{G}_{12} - G_{11}\exp(jk^-l)]\,, \qquad \text{(6)}$$

assuming that the influence of other than acoustic pressure fluctuations on the spectral estimates can be neglected. From which,

$$|\, p_1^+ \,| = (G_{11})^{0.5} / |\, 1 + \hat{R}_1 \,| \text{ and } p_1^- = \hat{R}_1 \hat{p}_1^+\,, \qquad \text{(7a, b)}$$

when the signal from transducer 1 is also chosen as a reference.

One should note that the effectiveness of the decomposition into $\hat{p}^{\pm}$ depends on the extent to which the spectral estimates $G_{11}, \hat{G}_{12}$ and G_{22} are contaminated by flow-induced pressure fluctuations p_s and any other signal acquisition or processing "noise". The method also relies on the differences between the acoustic pressure signals at positions 1 and 2. In a standing wave field the two signals are almost identical (equations (5a, b)), when $kl = n\pi$, with n any integer, so poor results can be expected when the spacing l is close to multiples of a half wavelength. On the other hand, due to the different propagation velocities, any influence of p_s on the spectral estimates of $\hat{G}_{12}$ will decrease as the distance l increases. Similarly, since p_s is generally random and uncorrelated with p_a, all three spectral estimates will more closely reflect the acoustic behaviour as the number of averages increases. A similar improvement occurs as the spectral analysis bandwidth is reduced. Clearly the most appropriate strategy will vary to some extent with application, depending on the spectral characteristics and strength of the acoustic field with its associated isentropic irrotational motion compared with that associated with the remaining disturbances convecting with the flow.

2.2 Pressure transducer calibration

It turns out [1, 7] that the net power flux is almost proportional to the magnitude of the imaginary part of $\hat{G}_{12}$. As shown in Figure 1, this may be close to zero over substantial ranges of the frequency spectrum, where adequate precision for the measurements of phase, among other factors, depends on the relative calibration of each transducer pair. If the measured transfer function $\hat{p}_2 / \hat{p}_1$ measured between two transducers (#1, #2) at positions 1 and 2 is $\hat{H}_A$, while after they were interchanged, including all signal path elements, the measurement yields $\hat{H}_B$, the required

calibration independent transfer function [1, 7] is then $H = \hat{H}_A^{0.5}\hat{H}_B^{0.5}$. This procedure can be repeated for each transducer pair in turn yielding relative transducer calibration data for the whole set. An absolute calibration of one of the set is required when absolute sound pressure levels are required.

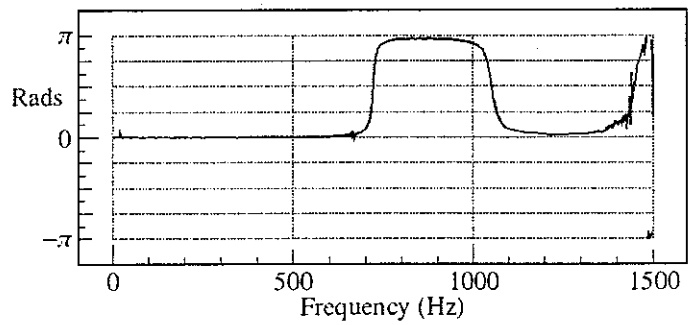

Figure 1 Phase of cross spectrum in exhaust tailpipe.

2.3 Experimental procedures

Laboratory tests at Southampton and bench tests at Bosal Afrika were mainly concerned with the development of robust procedures yielding reliable estimates of the net power flux [1] and coherent power flux [8], leading on to the identification [8] of flow noise sources. The acceleration tests at Bosal Afrika [9] concerned the application of order tracking and optimised sampling rate methods [9] to evaluate the acoustic properties of a system element in an industrial environment. As an approximation to the cyclic excitation during an acceleration test [1] a digitally generated slow sine sweep signal recorded on one channel of a digital tape recorder was used to excite the laboratory system. Ten minutes of data was recorded synchronously on the remaining seven channels for each run, and analysed with one Hz resolution with Hanning windowing and 50 percent overlap giving rise to 1200 process averages after analogue filtering with cut-off set to 1300 Hz. A representative individual record showing the analysis of one second of data appears in Figure 2, where the coherent acoustic signal stands some 20 dB above the background pressure fluctuations, although the corresponding signal to noise ratio of the signal records was 0 dB. Since the excitation frequency is known at any particular time, it is possible to exclude from the averaging process all frequencies except those within a narrow band centred on the excitation.

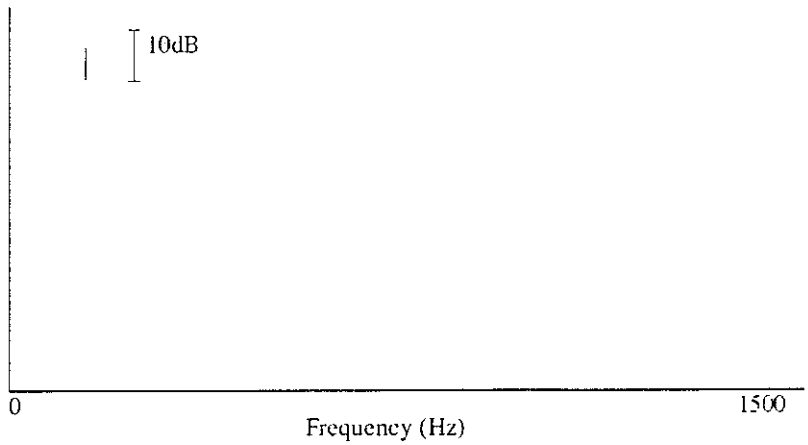

Figure 2 Single shot sample spectrum - only highlighted lines contribute to averaging - signal-to-noise ratio 0 dB.

The potential advantage of such selective averaging for identifying the acoustic behaviour of coherent signals buried in other flow induced pressure fluctuations is demonstrated in the comparison between the results with swept sine and with more conventional random excitation set out in Figure 3. The two transfer functions $\hat{H}_{12} = \hat{p}_2 / \hat{p}_1$ are very similar since the flow induced pressure fluctuations are sufficiently incoherent over the transducer separation path to cancel on average. However, the corresponding coherences are very different which explains the clear difference in the autospectra around 200, 770 and 1050 Hz, where elsewhere they remain similar. These results demonstrate that selective averaging provides a clear identification of the more coherent acoustic fluctuations even when their level lies below that of those generated by the flow.

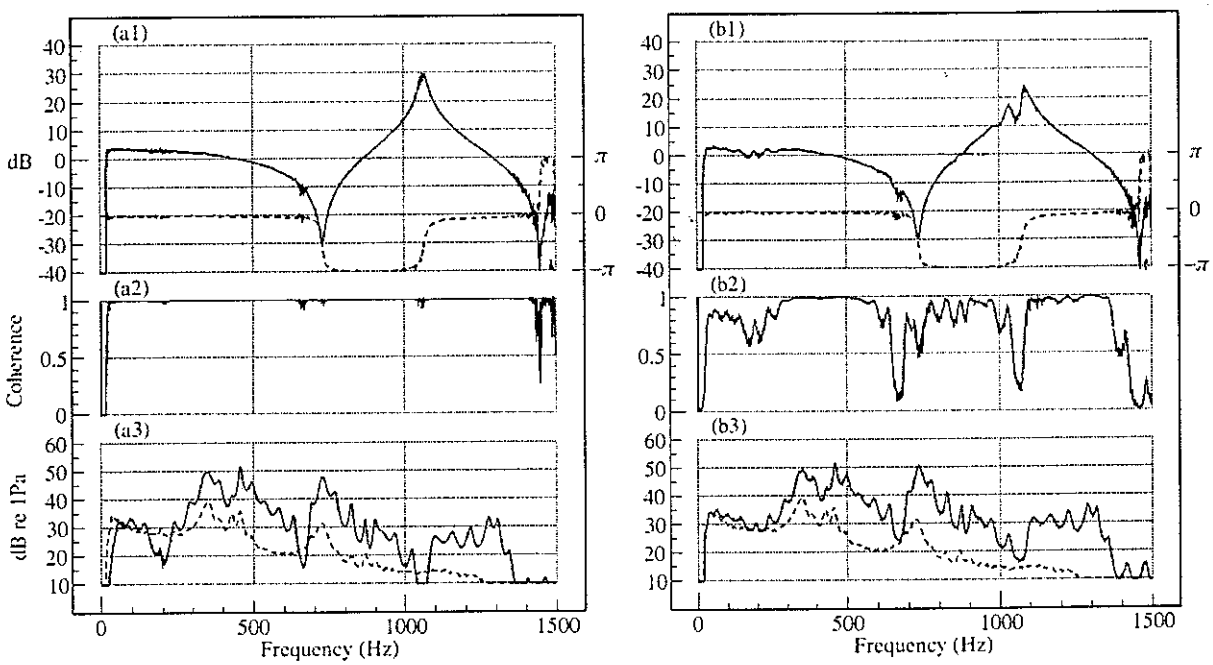

Figure 3 Comparison of measurements with flow Mach number 0.1. (a) With swept sine excitation and selective averaging; (b) with White noise excitation.
(1) Transfer function $\hat{H}_{12}$, — Mod - - Phase; (2) coherence; (3) autospectrum at microphone #1, — with acoustic excitation - - flow only.

The transfer function $\hat{p}_2 / \hat{p}_1$ may be calculated with the $\hat{H}_1$ estimator, $\hat{G}_{12} / G_{11} = \hat{p}_1^* \hat{p}_2 / \hat{p}_1^* p_1$, where * indicates the complex conjugate, or alternatively with the $\hat{H}_2$ estimator, $G_{22} / \hat{G}_{12}^* = \hat{p}_2^* \hat{p}_2 / \hat{p}_2^* \hat{p}_1$. With high coherence, both estimates should be closely similar. However, near standing wave minima, the corresponding signal to noise ratio of $\hat{p}_2$ may, for example, be significantly higher than that of $\hat{p}_1$. Substitution of the $\hat{H}_2$ estimator for the corresponding ratio $\hat{G}_{12} / G_{11}$ in equation (6) should then yield a "best" estimate for the reflection coefficient $\hat{R}_1$ at that frequency.

2.4 Experimental procedures with controlled engine acceleration

Currently, tailpipe orifice noise emissions spectra are measured during controlled acceleration or deceleration of the engine on a dynamometer to evaluate and then refine the exhaust system acoustic

performance. The results are normally displayed as engine order spectra against engine rpm, that are harmonically related to the firing frequency. With a four cylinder four stroke engine, the firing frequency occurs at 2E or twice the engine rotational frequency, while with six cylinders this is 3E and so on. With two stroke engines these values are doubled. Measurement of the individual contribution of each system element to the overall system acoustic performance clearly has a beneficial influence on the rate at which significant improvements are obtained during system refinement. Although the underlying principles are similar, the engine acceleration rather than the acoustic excitation is now the controlled variable, which requires [9] appropriate changes to the experimental and data processing procedures. The engine cyclic frequency, the mass flow and temperature all change systematically in time at some sweep rate that is never quite stationary and is also restricted by operating conditions, such as engine overheating. Standard order tracking [9] was adopted where the sampling frequency was synchronised with the instantaneous engine rotational speed and the time records and spectra represented respectively in revolutions and orders. Each record length contained an integer number of periods with the power of each harmonic component concentrated in an individual line. Special analogous procedures [9] were also developed to estimate the signal to noise ratios at each order in the pressure signal records, so as to obtain similar improvements in the identification of acoustic behaviour to those indicated in Figure 3.

2.5 Signal measurement

Electret microphones modified to operate up to sound pressure levels of 165 dB (Knowles, CA-8374) were used for the pressure measurements at Southampton, while water cooled Kistler type 701A quartz pressure transducers were used at Bosal Afrika. Measurements of flow temperature mean pressure and mass flow were also required to define the corresponding sound speed, and flow Mach number required for the calculations. The experimental layout and measured flow conditions during engine run up are illustrated in Figure 4. A similar arrangement was adopted at Southampton with a further pair of electrets mounted on the expansion chamber, with an additional one in free field near the open termination.

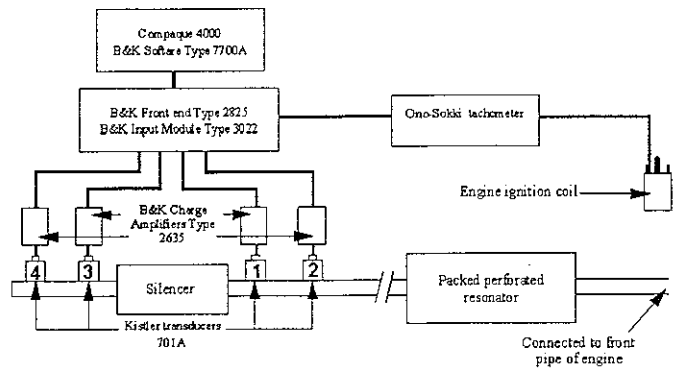

Figure 4(a) Experimental set up used for the measurements on the vehicle.

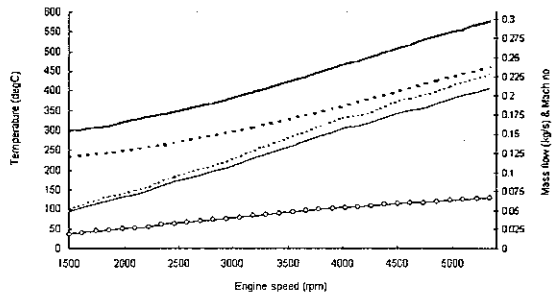

Figure 4(b) Mass flow (circles), inlet temperature (thick solid), outlet temperature (thick dash), inlet Mach number (thin dash) and outlet Mach number (thin solid) recorded for the Honda 1.5 litre during a full throttle run up on the chassis dynamometer.

3. DETERMINATION OF FLOW DUCT ACOUSTIC PROPERTIES

Some acoustic characteristics of flow ducts, such as reflection coefficients, impedance, and sound power flux spectra, can all be evaluated at some specific location [5] with the corresponding values of the incident and reflected component wave spectra $\hat{p}_n^{\pm}$. These relate to the axial reference position of say the transducer labelled $\#n$ of the local pair [1]. However, when the required behaviour concerns acoustic transfer across a duct element or section linking two lengths of pipe, such as in Figure 4, one also needs to establish the relative phase of the signals from the two pairs of transducers on the corresponding pipes. This can be determined [1] by calculating either the cross-spectrum $\hat{G}_{1n}$, or transfer function $\hat{H}_{1n}$ between the reference transducer $\#n$ of one pair and say #1 of the other. Then one can establish the required $\hat{p}_{n(\mathrm{ref})}^{\pm}$ from

$$\hat{p}_{n(\mathrm{ref})}^{\pm} = \hat{p}_n^{\pm} \frac{\hat{G}_{1n}}{(\hat{p}_1^{+} + \hat{p}_1^{-})^{*}(\hat{p}_n^{+} + \hat{p}_n^{-})} = \hat{p}_n^{\pm}\, \hat{H}_{1n} \frac{(\hat{p}_1^{+} + \hat{p}_1^{-})}{(\hat{p}_n^{+} + \hat{p}_n^{-})} \,. \qquad \text{(8a, b)}$$

Computer codes exist for predicting wave propagation along flow ducts, but it seems that they all rely to some extent on measurement to quantify acoustic sources, and aeroacoustic sources in particular [11, 12], when seeking to predict sound power emissions. However measurement of source independent properties, such as transfer functions, impedances and appropriately normalised sound power flux, can all be compared directly with predictions by appropriate existing codes [1]. One such experimentally validated linear acoustic code, APEX, developed by the second author [11, 12], proved suitable for this purpose.

3.1 Sound power measurements in strongly excited ducts

Sound pressure levels within industrial flow ducts may commonly exceed 160 dB, so that arguably, the assumption of linear acoustic behaviour ceases to be realistic. To investigate this, initial laboratory measurements were undertaken at corresponding sound pressure levels. Firstly, this was with a simple expansion chamber ten pipe diameters long with an area expansion ratio of 7.8, as

shown in Figure 1 of reference [1]. These proportions were chosen [4] to ensure that any contributions from aeroacoustic sources remained relatively small. The observed sound power flux in the exit pipe (or tailpipe) normalised by the incident power in the inlet (or downpipe) [1] compared closely with predictions obtained with APEX, as can be seen in Figure 5a. A sequence of such measurements gave similar results. Here the peaks in power flux at 360, 720, 1100 and 1460 Hz correspond to tailpipe acoustic resonances while those at 450, 900 and 1350 Hz correspond to chamber resonances.

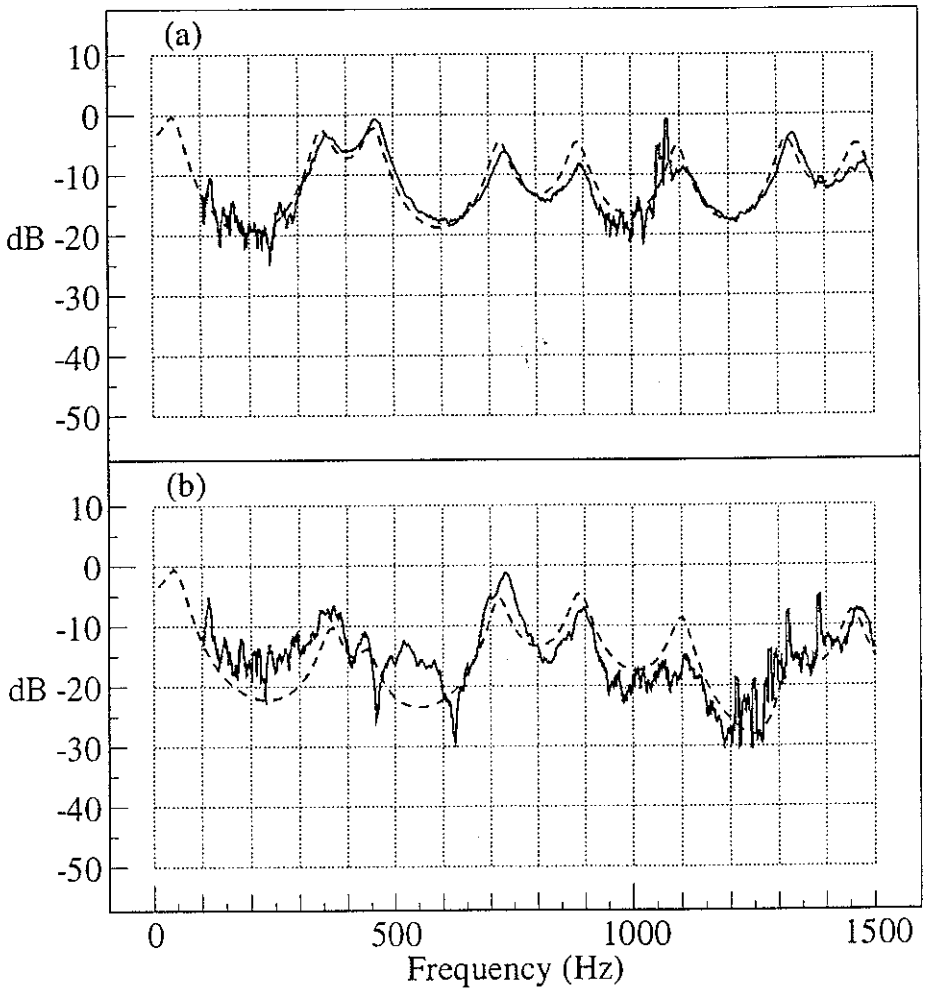

Figure 5 Normalised acoustic power flux in the tailpipe at Mach number $M = 0.2$, (a) low flow noise system, (b) high flow noise system; ——, measured; ----, predicted.

Similar comparisons in Figure 5b were obtained after the chamber had been modified by halving the length of the internal flow path to 5 diameters, resulting in a 20 fold increase [4] in the strength of aeroacoustic excitation by the mean flow. This was accomplished by inserting the tailpipe halfway into the chamber, as shown in Figure 2b of reference [8], to form an annular sidebranch [2, 5] at its outlet end. Reductions in sound power in excess of 10 dB at 450 and 1350 Hz corresponding respectively to the first two sidebranch resonances are clearly indicated in both observed and predicted results. Furthermore, the results in Figure 6 show that measurements of the radiated power have been in close agreement with predictions calculated [1] from the measured tailpipe flux. This is a result that was consistent with all those from several similar sets of experiments. Combined with existing experimental evidence [4, 6, 8], this demonstrates that the discrepancies between predictions and measurements in Figure 5b arise from nonlinear transfers between flow energy and sound energy

by aeroacoustic mechanisms [8]. These are directly associated with acoustically synchronised vortex shedding at an area expansion, leading to frequency dependent reverberant amplification or attenuation [4] of an incident sound field, thus giving rise to the observations recorded in Figure 5b. It is well known [2, 4], that such behaviour can be effectively eliminated by bridging between the inlet and outlet pipes of an expansion chamber with an acoustically transparent perforated pipe [4]. Its presence then suppresses periodic vortex formation. Such aeroacoustic mechanisms and their control is a topic of active research, but any representation of their acoustic influence is not currently included in the APEX code.

The experimental evidence also demonstrates that the assumption of linear acoustic wave motion models during the reduction of the experimental data was justified in the present context, at least for sound power measurements. To show this, one notes firstly, that the wave motion in an intake/exhaust flow duct represents a periodically excited, highly reverberent field, where propagating wave energy normally remains a small fraction of the total fluctuating energy. Secondly, that the peak to trough pressure ratio corresponding to a SPL of 165 dB is around 1.07, and that this pressure change is not a step, but is spread over a distance of some 0.5 m at the frequencies of interest. Finally, that this predominately standing wave motion exists in relatively short runs of uniform pipe, typically less than one or two metres long, bridging between area discontinuities. It is not surprising that the combined influence of all these relevant factors remains too small [11-14] for any significant wave steepening to occur within each pipe or system element. In such circumstances it is a reasonable assumption that acoustic models of wave propagation can still provide an adequate representation.

Furthermore, existing experimental evidence [15] suggests that acoustic models still provide a fair approximation to observed behaviour with continuous periodic excitation at pressure amplitudes that are at least an order of magnitude higher than those recorded in the sequence of experiments described here. Such facts leads one to speculate whether some discrepancies reported in the literature between observations and predicted flow duct acoustic behaviour, calculated with acoustic models, arise from inadequacies in the assumptions adopted in the acoustic modelling, rather than from wave steepening or similar physical factors. Among such [11-14], one can include the neglect of the existence of aeroacoustic sources or sinks [4-6, 8] at appropriate sites along the flow path, such as those whose influence is recorded in Figure 5b.

3.2 Flow excited sound fields

The measurements were repeated with the sound source switched off to identify the contributions from the aeroacoustic sources which were clearly audible. All the experimental evidence just described indicated that the coherent power flux represented the acoustic contribution [8] to the total power flux. The total and coherent power flux measured in the tailpipe of the simple chamber are compared in Figure 7. Comparisons with Figure 5a reveal that the tailpipe resonances at 360, 720 and 1100 Hz are clearly present as are the chamber resonances at 450 and 900 Hz. Clearer indications of these appear in the coherent power measurements indicating that the total power flux includes significant contributions from the pressure fluctuations convected with the flow. Such contributions are not evident with the excitation switched on, since the corresponding acoustic power was then increased by 30 to 40 dB, while both measured total and coherent power flux spectra are then closely similar, doubtless due to the selective averaging.

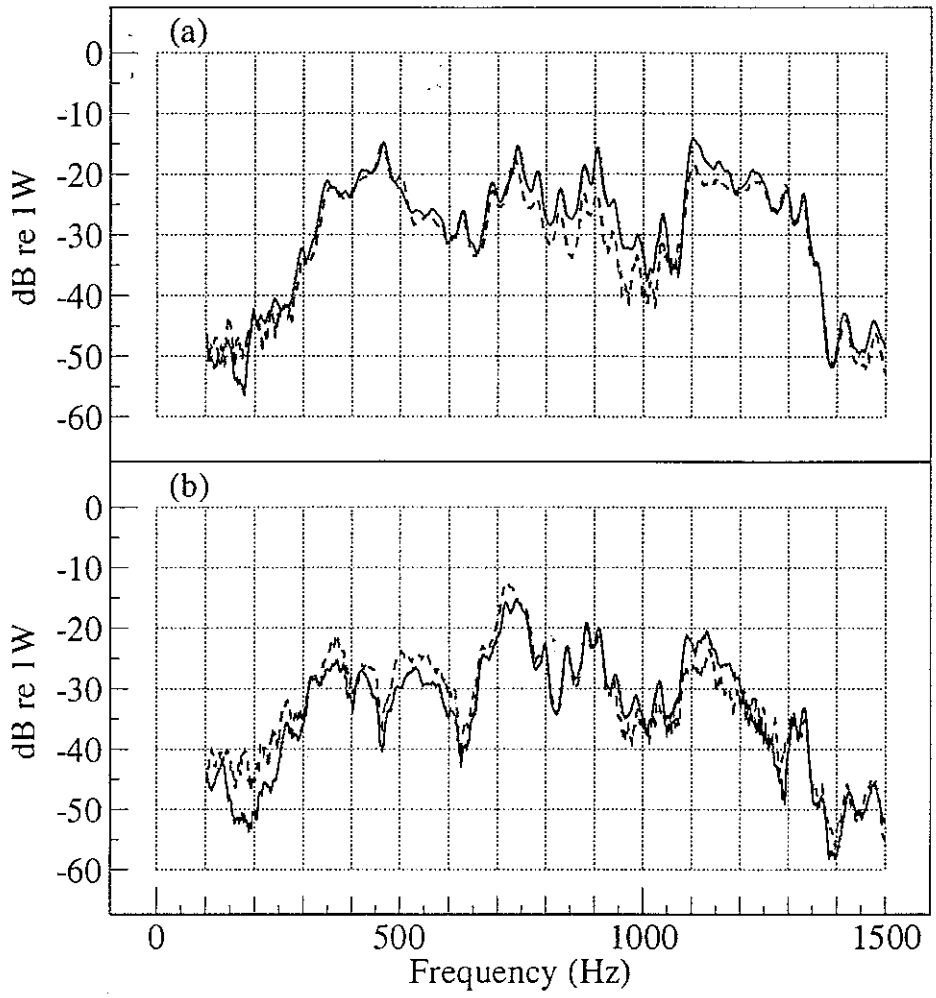

Figure 6 Radiated acoustic power at Mach number $M = 0.2$, (a) low flow noise system, (b) high flow noise system; ——, measured; ----, predicted from tailpipe power flux.

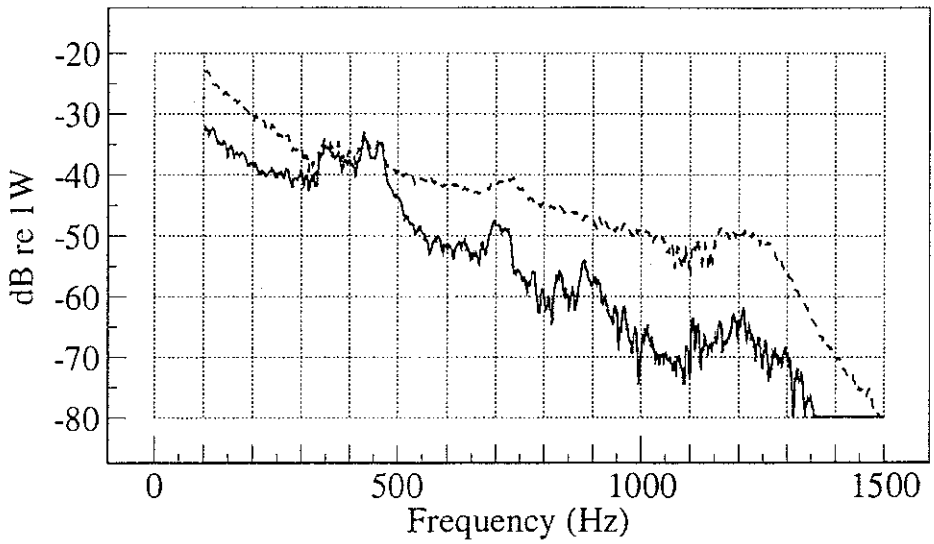

Figure 7 Measured power flux in tailpipe at $M = 0.1$, sound sources switched off; ——, coherent; ----, total.

Similar comparisons shown in Figure 8 were made for the "noisy" chamber. Here, the measured coherent radiated power is seen to be in close agreement with that predicted with the measured coherent tailpipe power flux [8] above 10^{-5} W and in fair agreement otherwise.

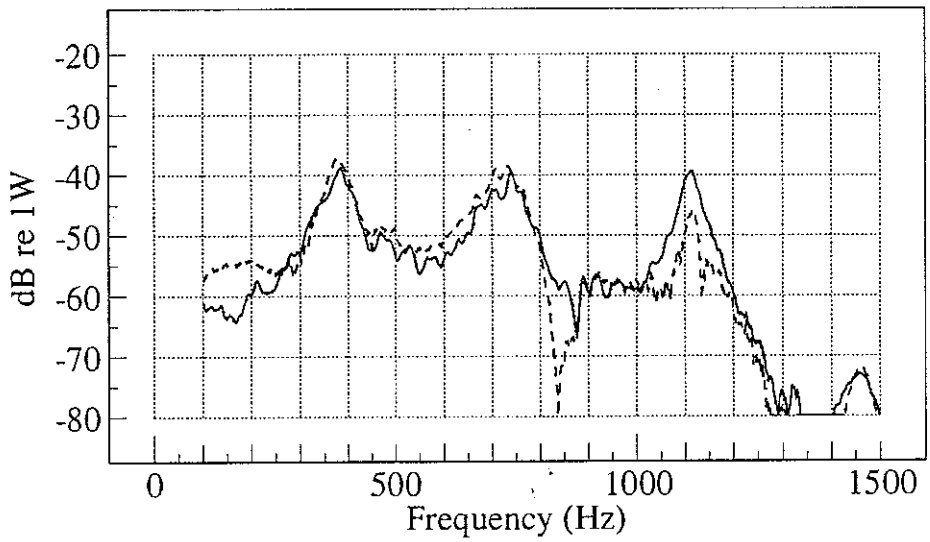

Figure 8 Radiated coherent power; with "noisy" chamber at $M = 0.2$; ——, measured in free field; ----, predicted from tailpipe power flux.

This result also implies that the coherent power flux measured in the tailpipe arises predominately from the acoustic pressure field. Furthermore, such measurements provide a useful procedure for identifying the acoustic contributions in a fluctuating pressure field with direct application to isolating and quantifying aeroacoustic sources. Comparison of the results in Figure 8 with the corresponding observations with excitation in Figure 6b reveals that the contributions to the radiated power spectrum arising from reverberant amplification of the incident sound fields are absent from Figure 8 as one would expect. See, for example, the reverberant increase of 10 dB between 500 and 600 Hz clearly present in both Figures 5b and 6b but not in Figure 8. Otherwise they indicate that there was now a relative drop in radiated sound power from 15 to 25 dB rather than 30 to 40 dB when the excitation is switched off, showing that the strength of the flow generated sources has been increased by 15 dB by halving the length of the free flow path in the expansion. A result in fair agreement with previous observations [4, 8].

3.3 Vehicle measurements and predictions

The exhaust measurements [9] were performed at constant acceleration on vehicle dynomometer at a controlled sweep rate of 30 rpm/sec. The relevant signal processing used 0.025 order resolution, 75 percent overlap with a Hanning window, providing five averages over the measurement interval for each record. The order tracking was synchronised with the tachometer and the corresponding measured flow conditions (Figure 4b) were employed for the power flux and other acoustic calculation with each record. Special precautions were taken when possible to avoid positioning the transducers at or near standing wave minima, particularly in the tailpipe. Appropriate additions and adjustments were also made to the APEX prediction code, to equip it for following the changing flow conditions during acceleration. A typical set of sound power flux measurements for the first four orders [9] are compared with the corresponding predictions in Figure 9. The results show close agreement between measured and predicted power flux at the resonant peaks. These spectral regions are obviously of the greatest practical significance for noise emission predictions.

The rather localised discrepancies elsewhere in the spectra seem to be correlated [9] with low signal to noise ratios at one or more of the pressure transducers. The sound pressure levels for each of the first four orders recorded at transducer #1 during run up are plotted in Figure 10. These exhibit systematic fluctuations of 20 to 30 dB, a feature presumably associated with wave interference and the resulting standing wave maxima and minima. Similar fluctuations in level were present [9] at the other transducer positions. Other measured characteristics [9], such as acoustic attenuation spectra, showed better agreement with prediction as one might expect, since signal contamination by flow disturbances [1] then tends to cancel.

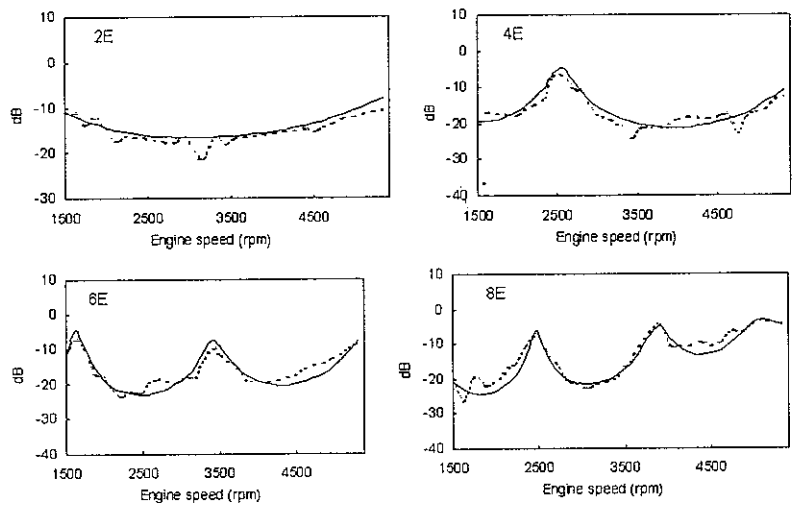

Figure 9 Measured (thin dash) and predicted (solid) normalised acoustic power flux in the outlet pipe for a full throttle run up of the Honda 1.5 litre.

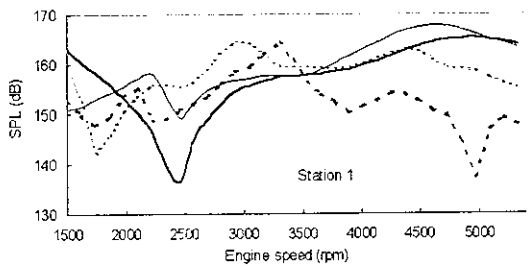

Figure 10 Sound pressure orders measured at station #1 for the Honda 1.5 litre during a full throttle run up on the chassis dynamometer, 2E (thick solid), 4E (thin solid), 6E (thin dash), 8E (thick dash).

4. DISCUSSION

The results summarised in this paper demonstrate several of the problems associated with the estimation of sound power flux in flow duct systems, such as those arising from poor signal to noise ratios associated with the existence of turbulent pressure fluctuations in combination with acoustic standing waves. The consequences of their presence may be tolerable when considering global system properties, such as pressure transfer functions, but further processing of the data records to yield robust estimates of acoustic power flux reveals the need for techniques providing greater experimental precision for these measurements. The success of swept-sine [1] or swept periodic excitation [9] combined with appropriate selective averaging in reducing such problems is demonstrated by the material presented here. With uncontrolled excitation, such as that induced by the flow, it has also been shown that coherent power flux measurements [8] can be closely identified with the acoustic contribution to the total power flux and thus assist in the evaluation of aeroacoustic sources, [8]. In both cyclically and flow excited situations the results confirm that the assumptions involved in the derivation of equations (6) and (7) remain appropriate even when boundary layer and other flow induced pressure fluctuations are present.

The experimental evidence presented here also demonstrates that data reduction, based on the one dimensional linear acoustic models, can provide realistic descriptions of the acoustic characteristics of cyclicly excited flow duct systems and their elements, up to sound pressure levels in excess of 165 dB! With flow excited systems the maximum sound pressure levels recorded were around 20 dB lower than this, although the corresponding overall fluctuating pressure levels were still close to 160 dB. Acoustic characteristics calculated with linear acoustic models [1, 8, 9] were also found to be in good agreement with the measurements, indicating that wave steepening is not yet a significant factor at these conditions of these experiments.

References

1. K R Holland and P O A L Davies 2000 *Journal of Sound and Vibration* **230**(4), 915-932. The measurement of sound power flux in flow ducts.
2. P O A L Davies 1996 *Journal of Sound and Vibration* **190**(4), 677-712. Piston engine intake and exhaust system design.
3. C L Morfey 1971 *Journal of Sound and Vibration* **14**(2), 159-170. Acoustic energy in non-uniform flows.
4. P O A L Davies 1981 *Journal of Sound and Vibration* **77**(2), 191-209. Flow-acoustic coupling in ducts.
5. P O A L Davies 1988 *Journal of Sound and Vibration* **124**(1), 91-115. Practical flow duct acoustics.
6. P O A L Davies 1996 *Journal of Sound and Vibration* **190**(3), 345-362. Aeroacoustics and time varying systems.
7. J V Chung and D A Blaser 1980 *Journal of the Acoustical Society of America* **68**, 1570-1579. Transfer function method of measuring acoustic intensity in a duct system with flow.
8. P O A L Davies and K R Holland 2001 *Journal of Sound and Vibration* (in press). The observed aeroacoustic behaviour of some flow-excited expansion chambers.
9. D C van der Walt 2001 *Journal of Sound and Vibration* (in press). Measurement technique to assess the acoustic properties of a silencer component for transient engine conditions.
10. R Ramakrishnan 1980 *Journal of Sound and Vibration***72**(4), 554-558. A note on the reflection coefficients of higher duct modes.

11. P O A L Davies and M F Harrison 1997 *Journal of Sound and Vibration* **202**(2), 249-274. Predictive acoustic modelling applied to the control of intake/exhaust noise of internal combustion engines.
12. P O A L Davies and K R Holland 1999 *Journal of Sound and Vibration* **223**(3), 425-444. IC Engine intake and exhaust noise assessment.
13. R J Alfredson and P O A L Davies 1970 *Journal of Sound and Vibration* **13**(4), 389-408. The radiation of sound from an engine exhaust.
14. R J Alfredson and P O A L Davies 1971 *Journal of Sound and Vibration* **15**(2), 175-196. The performance of exhaust silencer components.
15. E A A Yaseen and P O A L Davies 1998 *Journal of Sound and Vibration* **124**(3), 586-59. Finite interfering waves in continuously excited open pipes.